Short Communication

Journal of RAMAN SPECTROSCOPY

Received: 27 July 2008 Accepted: 10 August 2008 Published online in Wiley Interscience: 15 December 2008

(www.interscience.wiley.com) DOI 10.1002/jrs.2120

Characterisation of carbonaceous materials using Raman spectroscopy: a comparison of carbon nanotube filters, single- and multi-walled nanotubes, graphitised porous carbon and graphite

H. M. Heise,[a] R. Kuckuk,[a] A. K. Ojha,[b†] A. Srivastava,[c] V. Srivastava[d] and B. P. Asthana[c*]

Multi-walled carbon nanotube (MWCNT) filters have been recently synthesised which have specific molecular filtering capabilities and good mechanical strength. Optical and scanning electron microscopy (SEM) reveals the formation of highly aligned arrays of bundles of carbon nanotubes having lengths up to 500 μm. The Raman spectra of this material along with four other carbonaceous materials, commercially available single-walled carbon nanotubes (SWCNTs) and MWCNTs, graphitised porous carbon (Carbotrap) and graphite have been recorded using two-excitation wavelengths, 532 and 785 nm, and analysed for band positions and shape with special emphasis paid to the D-, G- and G′-bands. A major difference between the different MWCNT varieties analysed is that G-bands in the MWCNT filters exhibit almost no dispersion, whereas the other MWCNTs show a noticeable dispersive behaviour with a change in the excitation wavelength. Spectral features similar to those of the MWCNT filter varieties were observed for the Carbotrap material. From the line shape analysis, the intensity ratio, I_D/I_G, of the more ordered MWCNT filter material using the integral G-band turns out to be two times lower than that of the less ordered MWCNT filter product at both excitation wavelengths. This parameter can, therefore, be used as a measure of the degree of MWCNT alignment in filter varieties, which is well supported also by our SEM study.

Keywords: carbonaceous materials; multi-walled carbon nanotube (MWCNT) filters; Raman spectroscopy; D- and G-band analysis; optical and scanning electron microscopy (SEM)

Introduction

Carbon is one of the most abundant elements in the universe and shows different forms according to the electron hybridisation, which results in different type of bonding between the carbon atoms. The lattice dynamics and vibrational spectroscopy of sp^2 carbon materials have been the subject of numerous investigations and some representatives (Refs [1–6)] are cited here. Raman spectroscopy has been an important tool in investigating such materials because their spectrum is particularly sensitive to the microstructure of the carbon. Raman scattering from carbons is always a resonant process, in which those configurations whose band gaps match the excitation energy are preferentially excited. Any mixture of sp^3, sp^2 and sp carbon atoms may have a band gap between 0 and 6 eV. Fortunately, this energy range matches with electromagnetic radiation in the infrared, visible and ultraviolett (IR-VIS-UV) regions and hence these materials are well suited for a Raman study using almost any excitation wavelength, thereby making a dispersion study quite conveniently feasible.

Besides graphite and diamond, the discovery of fullerenes and subsequently of carbon nanotubes (CNTs) added a new dimension in carbon science. CNTs are long, cylindrical molecules consisting of a circular array of nearly sp^2 hybridised carbon atoms. The well-known CNTs prepared in the past have been classified as single-walled nanotubes (SWNTs)[6–8] and multi-walled nanotubes (MWNTs)[9] with each tube embedded within a larger tube. Usually, SWNTs show diameters of approximately 1 nm and a length of 1–100 μm. In an interesting article, the relationship of CNTs to other carbon materials has been discussed by Dresselhaus and Endo.[10] Many different methods exist to grow CNTs and the most widely used techniques are arc discharge, laser furnace, and chemical vapour deposition (CVD), which have been reviewed recently.[11,12] Large aligned-nanotube bundles from ferrocene pyrolysis have been reported by Rao *et al*.[13] A special variety

* *Correspondence to: B. P. Asthana, Department of Physics, Banaras Hindu University, Varanas-221005, India. E-mail: bpasthana@rediffmail.com*

† *On leave from the Department of Physics, Motilal Nehru National Institute of Technology, Allahabad-211004, India.*

a *ISAS - Institute for Analytical Sciences at the University of Dortmund, D-44139 Dortmund, Germany*

b *School of Engineering and Science, Jacobs University Bremen, D-28759 Bremen, Germany*

c *Department of Physics, Banaras Hindu University, Varanas-221005, India*

d *Department of Ceramic Engineering, Institute of Technology, Banaras Hindu University, Varanas-221005, India*

of CNTs of relatively larger length forming macroscopic hollow cylinders with radially aligned CNT walls has been reported by Srivastava *et al*.,[14] which have been successfully used as filters for compound separation. Intricate applications like filtering a bacterial pollutant and compounds with high octane number from gasoline suggest that these nanotubes are suitable for industrial applications.

In recent years, Raman spectroscopy has been used as a powerful tool to characterise different types of carbonaceous materials, especially in the case of CNT varieties. Besides Raman spectra, UV-VIS-NIR spectra also of individual single-walled carbon nanotubes (SWCNTs) were recorded by Thomsen and Reich[15] and interpreted for electronic excitations existing in various types of tubes. Reviews on Raman spectroscopy of isolated SWCNTs have recently been published by Dresselhaus *et al*.[6,16] The basic concepts and characteristics of Raman spectra from CNTs, both isolated and bundled, that were based on studies by resonance Raman scattering, have been presented by Jorio *et al*.[17] A Raman spectroscopic method has been recently devised for analysis of mixtures of SWCNTs and multi-walled carbon nanotubes (MWCNTs), which also gives a detailed description of the spectral differences observed for both carbon varieties.[18] Because of the large diameters of MWCNTs, containing also an ensemble of nanotubes with varying diameters, most of the characteristic differences observed for SWCNT spectra, when compared to those of graphite and similar materials, are not so evident for MWCNTs. The Raman spectroscopy of MWCNTs has not been well investigated up to now, which is a recent observation by the Dresselhaus group.[6] In view of this fact, the Raman spectra of our radially aligned MWCNT filter varieties may give further insight into the spectra-structure correlation.

Besides the use of MWCNT as filters, such materials have also been brought into play as a sorbent phase for separation techniques (as described in the recent review by Valcárcel *et al*.[19]). When contemplating on their adsorption characteristics, we also included a variety of porous graphitised carbon black in our study. Graphitised carbon-based adsorbents are commercially available under the trade names Carbopack and Carbotrap, whereas carbon molecular sieves are available, e.g. under Carbosieve (all from Supelco, Bellefonte, PA). The carbon molecular sieves consist of a carbon skeletal framework that remains after pyrolysis of a polymeric precursor. The carbon molecular sieves are designed to trap smaller, more volatile compounds while the graphitised carbon blacks are better suited for larger, less volatile compounds. Other ordered and disordered mesoporous carbons, with similar microporosity and surface properties as those of graphitised carbon black Carbopack, were recently prepared and investigated by Raman spectroscopy, giving evidence for the increased sp^2 carbon structures.[20] Other carbonaceous materials such as carbon blacks and soot have recently been found interesting by using Raman spectroscopy at different laser excitation wavelengths, which included a band analysis.[5] With regard to the reactivity of carbonaceous materials, a Raman spectroscopic study of ordered and disordered carbon varieties such as coke and charcoal was studied recently.[4] Tan *et al*.[21] presented a review on the Raman study of several different and less-common non planar graphite materials, where the polarisation properties related to the structural features, line shape of first-order dispersive mode and its combination modes, variation of wavenumber and other unique features were discussed and some of the new features were explained using the double resonance mechanism. Thomsen *et al*.,[22] in another review, identified six criteria which help in understanding the role of the double resonance process, and they applied these criteria to the experimental results for the radial breathing mode (RBM) and the D mode. Kneipp *et al*.[23] exploited the effect of surface enhanced Raman scattering (SERS) when the SWCNTs were in contact with silver or gold nanostructures, where the Raman signal could be enhanced by up to 14 orders of magnitude, which allowed a measurement from even a single SWCNT.

In view of the earlier studies and foregoing discussions, it was thought worthwhile to take up the task of a rather complete characterisation of CNT filters from a Raman spectroscopic point of view in relation to the spectra of other related carbonaceous materials. In this study, besides Raman spectra recorded with different laser excitation wavelengths, we also present optical, scanning electron microscopy (SEM) and high-resolution transmission microscopy (HRTEM) micrographs, which give a clear idea regarding the degree of nanotube alignment and their graphitisation. In contrast to this, the porous structure in the graphitised carbon black is also evident from its SEM study. Despite the fact that many papers have been published on the structural analysis by vibrational spectroscopy, a universal evaluation method has not yet been developed for carbonaceous materials with widely differing structures. However, with this contribution some additional insights are obtained.

Experimental

Materials

Macro-scale hollow carbon cylinders up to a few centimetres in diameter and several centimetres long consisting of MWCNT filters with diameters ranging from 20 to 50 nm thickness were synthesised using a continuous spray pyrolysis method with a spray of ferrocene-derived iron particles acting as the catalyst. The nanotubes grow in radial directions on the walls of removable silica tube templates leading to the formation of freestanding and continuous hollow cylindrical tubes made up of MWCNTs.[14] In this reaction, ferrocene breaks and gives nano-clusters of free iron particles, which function as a catalyst for the growth of CNTs. One of the important features of CNTs synthesised by using a ferrocene-benzene precursor is that they are produced in high yield (1.25 g/run). It was found that the optimum concentration of ferrocene in benzene for the long-length nanotubes is 5 mg/ml. The two abbreviations of MWCNTI and MWCNTII used hereinafter in our entire presentation and discussion stand for the filter variety grown through spray pyrolysis technique. The optical image from a powdered MWCNT sample and the SEM as well as the HRTEM micrographs of the MWCNT filter varieties are shown in Figs 1 and 2, where the second batch shows a reduced alignment of the individual tubes, which is obvious from the SEM micrographs. The inner and outer diameters of the MWCNT filter varieties are ~15 and ~30 nm, respectively, as determined by the transmission electron microscopy (TEM) study.

For a comparative study, some other CNTs were purchased from Aldrich (Milwaukee, WI, USA). The SWNTs were procured from CarboLex, Inc. of Lexington (Kentucky, USA). The batch quantity (product # 519308) obtained was of AP-grade (as-prepared, i.e. non-chemically purified), which consisted of bundles of SWCNTs with 10–200 individual nanotubes per bundle with an average diameter of 1.2–1.5 nm and a bundle length of ~20 μm. The purity of the AP-grade was stated to range between 50 and 70% by volume, as determined by Raman spectroscopy and SEM. Major impurities as mentioned by the manufacturer were carbon

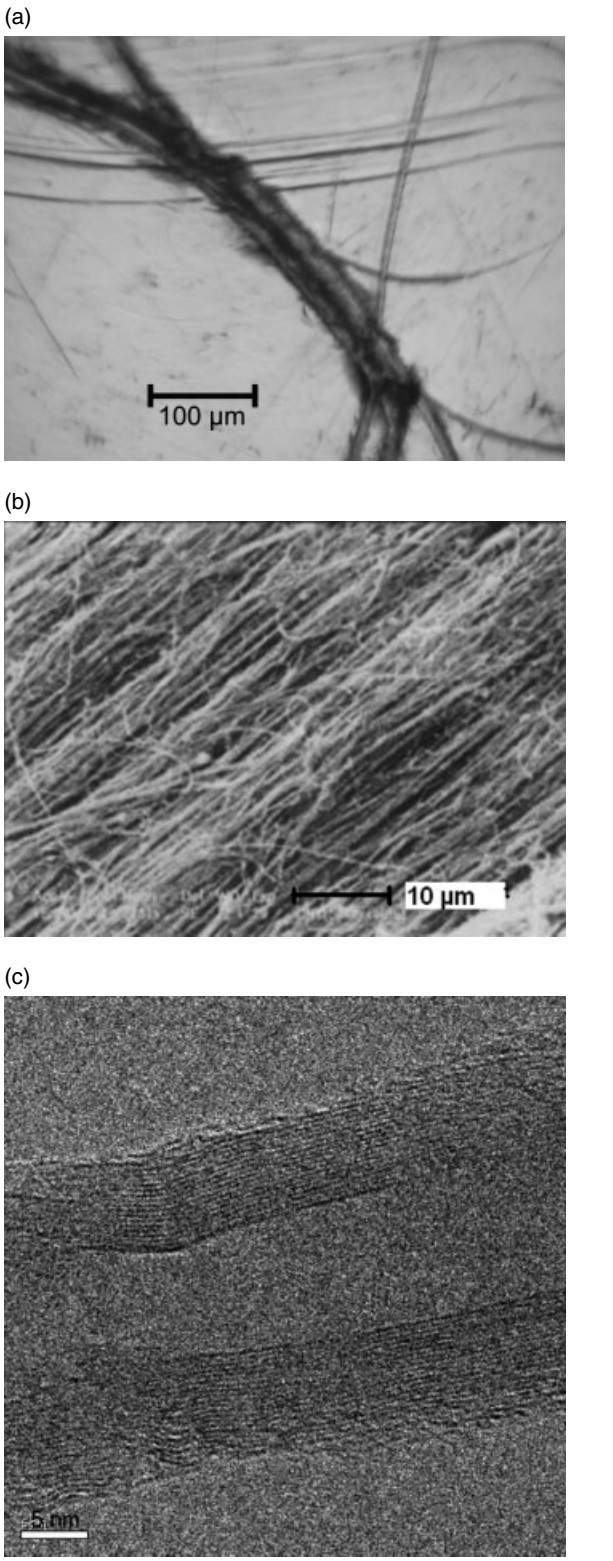

Figure 1. (a) Optical micrograph of aligned multi-walled carbon nanotubes (MWCNT filter); (b) SEM micrograph showing aligned multi-walled carbon nanotubes (MWCNT filter); (c) HRTEM micrograph showing one multi-walled carbon nanotube (MWCNT filter) having well graphitised walls (nearly 20 walls with an average wall separation of 0.34 nm; bar length 5 nm).

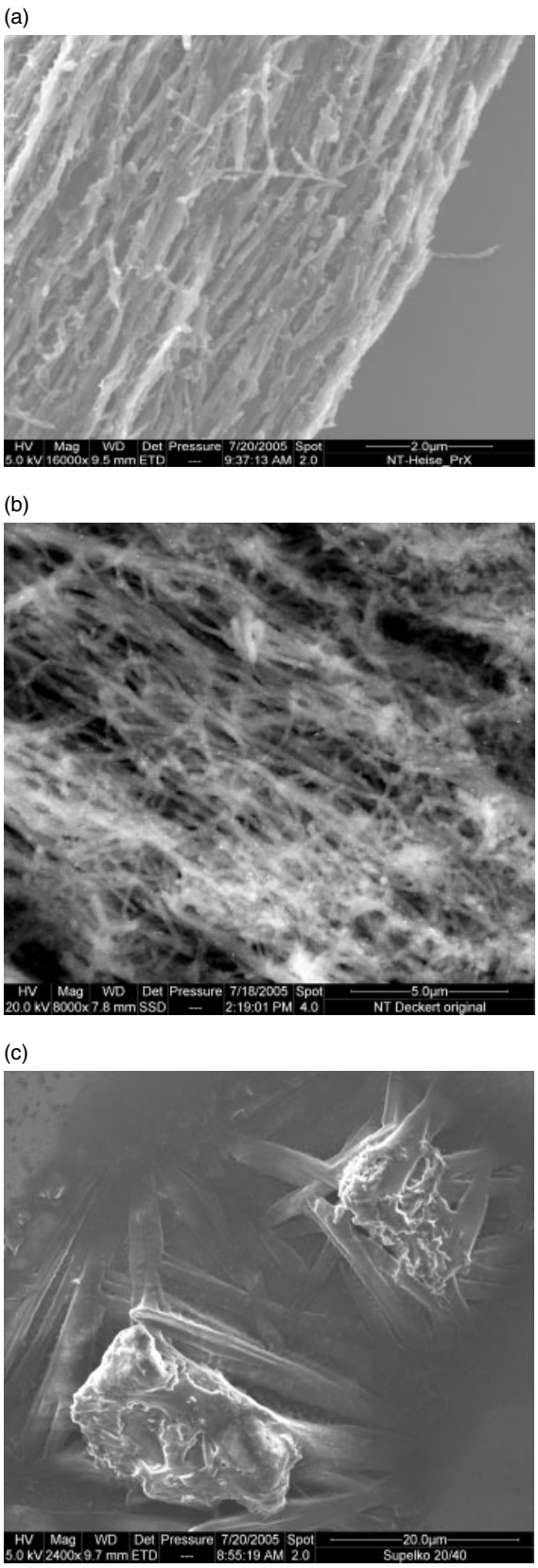

Figure 2. SEM micrographs of (a) MWCNTI filter; (b) MWCNTII filter; and (c) Carbotrap.

Journal of RAMAN SPECTROSCOPY

nanospheres and carbon-encapsulated catalyst nanoparticles. The second SWCNT material (product # 636797) was characterised having a mean diameter of 1–2 nm, as determined by HRTEM. Purity was analysed by energy dispersive X-ray spectroscopy and a SWCNT content >50% with an average outside diameter of 1.1 nm and a length of 0.5–100 μm (the extent of impurities as quoted could be amorphous carbon: ~3%, other nanotubes: ~40%) was reported by the manufacturer.

We also procured MWCNTs from Aldrich for which Raman spectra were recorded. These MWCNTs had the following characteristics: batch 1 (O.D. × I.D. × length = 30–50 nm × 5–15 nm × 0.5–200 μm; carbon content >95%) and batch 2 (O.D. × I.D. × length = 10–20 nm × 5–10 nm × 0.5–200 μm; carbon content >95%) with a purity determined by thermogravimetric analysis. Since the spectra of the two batches did not show any significant differences, the data for only the second batch are presented and further discussed. The abbreviation of MWCNT as used later in our tables and diagrams stands for the species procured from Aldrich, whereas MWCNTI and MWCNTII refer to two batches of synthesised MWCNT filters. Other materials selected for a comparative study were pure graphite and Carbotrap 20/40 mesh from Supelco, Bellefonte (PA, USA). The SEM micrograph of Carbotrap along with those of the filter varieties (MWCNTI and MWCNTII) are shown in Fig. 2. The material, a graphitised carbon black, is commonly used as adsorbent for trapping trace volatile organic pollutants ranging from C4/C5 compounds to substances of medium volatility. We have concentrated our Raman studies on the band analysis of five materials: MWCNT filter, another MWCNT variety (batch 2), one set of SWCNT (procured from Aldrich, product # 636797), graphite and Carbotrap.

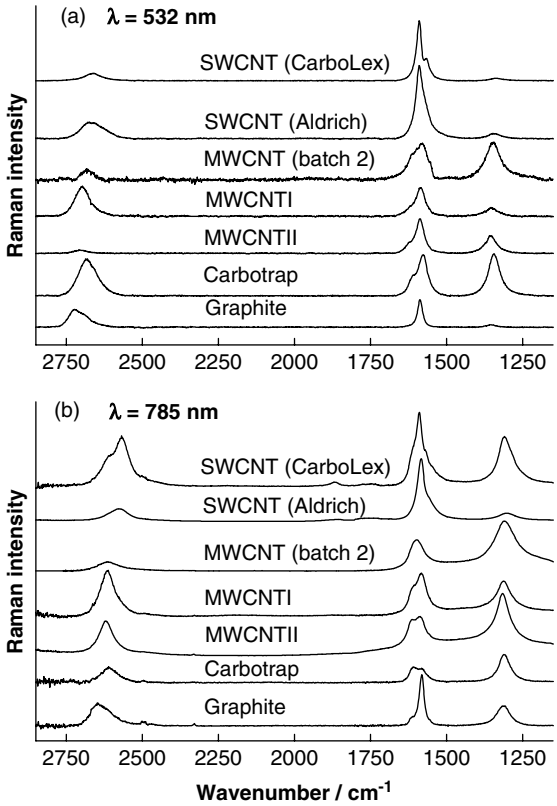

Figure 3. Raman spectra of various carbonaceous materials in the range 2800–1200 cm^{-1} with (a) 532 nm and (b) 785 nm excitation wavelength, respectively.

Optical and scanning electron microscopy

For optical microscopy, we used an infrared microscope (IR-microscope) (model Auto IMAGE) for transmission measurements attached to a Perkin-Elmer – 2000 Fourier transform infrared (FTIR) spectrometer (Perkin-Elmer, Überlingen, Germany). The scanning electron microscopic study was made using a SEM (model-XL20) from Philips Instruments (Eindhoven, The Netherlands). The HRTEM study was carried out using a model JEM-3010 from JEOL Ltd (Tokyo, Japan).

Raman measurements

For Raman measurements, two different spectrometers with two different excitation wavelengths were used. The XY-Dilor Raman spectrometer (HORIBA Jobin Yvon GmbH) is a dispersive research Raman spectrometer. It consists of a triple 0.5 m monochromator and uses the frequency-doubled radiation from a Nd-YAG laser (excitation wavelength of 532 nm with 500 mW) and a liquid nitrogen cooled charge-coupled device (CCD) (from Wright Instruments Ltd) for detection. The measurements in the present study were carried out using a slit width of 100 μm with an integration time of 1000 s and 25 spectral frame accumulations. A confocal Raman microscope is coupled to the Raman spectrometer, providing spectra from sample spots down to about 1 μm^2, which can be used for the analysis of composition and structure of small particles, inclusions or material defects.

Further measurements were carried out using a diode laser based Raman system, which was a portable HoloSpec Raman spectrometer from Kaiser Optical Systems, Inc., equipped with a diode laser (λ = 785 nm, 50 mW) from SDL, Inc. and a liquid-N_2 cooled CCD detector from Roper Scientific, Inc. The spectrometer uses a non-scanning polychromator and is equipped with a fibre-optic probe, usable also for remote-measurements. An integration time of 25 s with 10 spectral frame accumulations was employed for recording the spectra in the present study at a laser power of 10 mW. The samples were placed in a cup used for Raman spectroscopy of powdered samples.

Results and Discussion

Optical, SEM and HRTEM studies

The optical images from a powdered MWCNT (filter) sample as shown in Fig. 1(a) are able to suggest the long length and superior alignment of carbon nanostructures. One can see a bundle of MWCNTs which is further divided into subsequent branches of nanotube bundles. It is further confirmed by SEM investigation that highly aligned bundles of nanotubes are formed, the typical length reaching up to 500 μm. Figure 1(b) reveals a highly organised, self-aligned growth of CNTs. It is also clear from this micrograph that the density of the aligned CNTs is very high. Along with these bundles that are clean and free from other impurity materials, some flakes of aligned CNTs are also formed. SEM micrographs from the two filter batches including that of a Carbotrap sample are shown in Fig. 2.

In order to confirm the formation of MWCNT in the filter samples, HRTEM has also been carried out. A typical high-resolution micrograph of a MWCNT is shown in Fig. 1(c). The micrograph illustrates that the inner and outer diameters of the MWCNT are

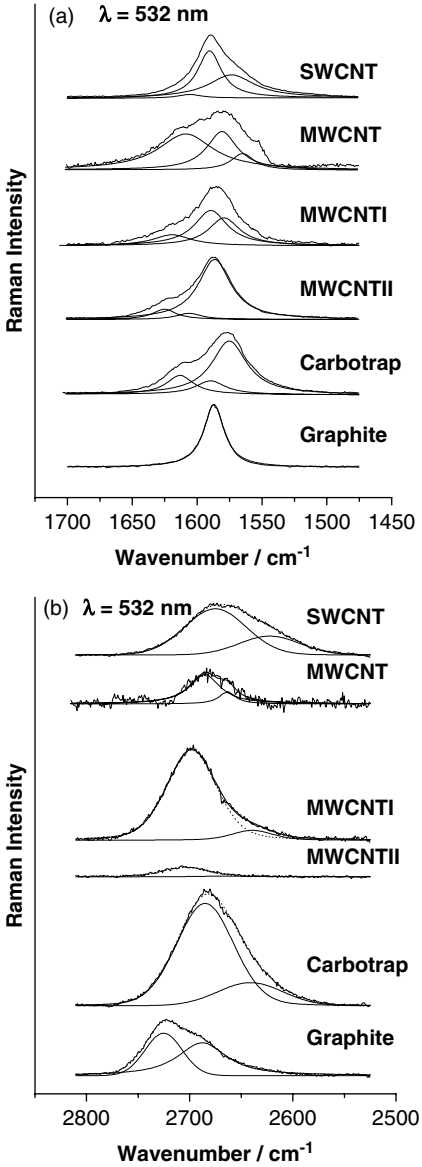

Figure 4. Raman spectra of various carbonaceous materials (SWCNT from Aldrich, product #636797) with 532 nm excitation wavelength along with the fitted band components; (a) in the range 1700–1475 cm^{-1} and (b) in the range 2800–2525 cm^{-1}.

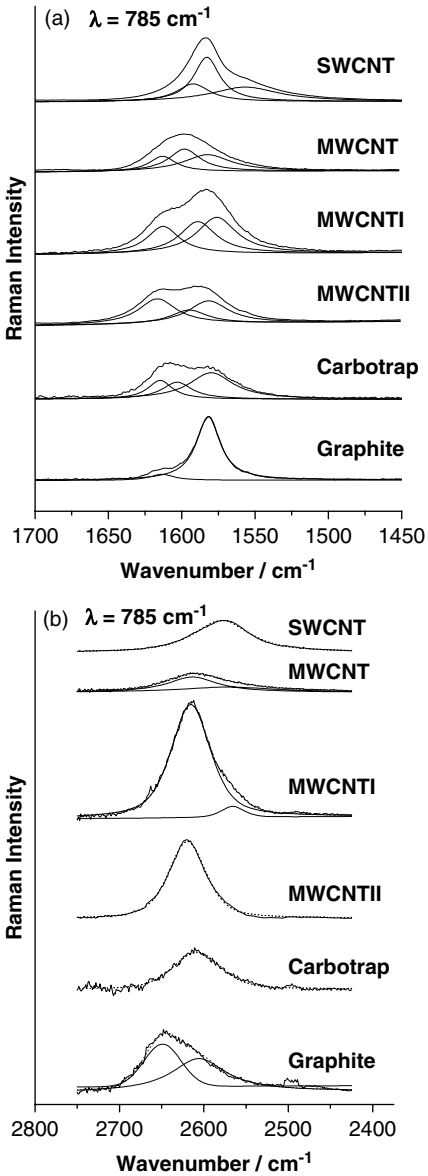

Figure 5. Raman spectra of various carbonaceous materials (SWCNT from Aldrich, product #636797) with 785 nm excitation wavelength along with the fitted band components: (a) in the range 1750–1450 cm^{-1} and (b) in the range 2750–2425 cm^{-1}.

~15 and ~30 nm, respectively. Nearly 20 walls on each side of the core of the CNT, the neighbouring walls separated by 3.4 Å, are seen and they form the coaxial graphitic cylinders.

Raman spectra and line shape analysis

The Raman spectra of different carbonaceous materials recorded using the two laser excitation wavelengths of 532 and 785 nm are presented in Fig. 3(a) and (b) in the entire region, 2800–1200 cm^{-1}. The spectra of the materials, i.e. SWCNTs from Aldrich, the two MWCNT filter varieties (abbreviated by MWCNTIs, MWCNTIIs), a MWCNT sample from Aldrich, Carbotrap and graphite, were investigated in more detail within two different regions, 1750–1450 and 2800–2400 cm^{-1}. Experimentally recorded spectra at the two-excitation wavelengths, 532 and 785 nm along with the fitted spectra, are presented in Figs 4 and 5, respectively. The spectra in the region of 1750–1450 cm^{-1}, shown in Figs 4(a) and 5(a), were fitted using a least-squares method taking three peaks, while the spectra in the region, 2800–2400 cm^{-1}, as illustrated by Figs 4(b) and 5(b), were analysed taking two peaks into account. The discussion of our results will include, where appropriate, a detailed description of the theoretical modelling and interpretation of SWCNT spectra as previously reported in the literature.

Raman D-band and degree of alignment in MWCNT bundles

The weak bands at ~1342 and 1301 cm^{-1} in the spectra of SWCNT from Aldrich recorded using 532 and 785 nm excitation, respectively, are assigned as D-bands (D for 'disorder'). However, more prominent bands can be found for the remaining materials (Fig. 3). The D-band positions corresponding to all five materials mentioned above are presented in Table 1. The positions of the

Table 1. Peak positions, linewidths (FWHM) and band integrals of the D-band of different carbonaceous materials[a] with two-excitation wavelengths

	$\lambda = 532$ nm			$\lambda = 785$ nm		
Sample	ω (cm^{-1})	Width (cm^{-1})	Intensity (arb. units)	ω (cm^{-1})	Width (cm^{-1})	Intensity (arb. units)
SWCNT	1343	54	3.8	1301	68	9.5
MWCNT	1347	54	79	1308	78	97.4
MWCNTI	1352	55	17.2	1312	54	53.4
MWCNTII	1354	44	29.1	1316	52	67.9
Carbotrap	1344	46	57.1	1310	46	55.5
Graphite	1354	42	3.78	1314	53	25.7

[a] For the individual CNT dimensions, see the Experimental Section.

D-peaks in the spectra of MWCNT, MWCNTIs, MWCNTIIs, Carbotrap and graphite recorded using 532 nm excitation are 1347, 1352, 1354, 1344 and 1354 cm^{-1}, respectively. The positions of the D-peaks in the spectra of these substances recorded using 785-nm excitation wavelength are found at 1308, 1312, 1316, 1310 and 1314 cm^{-1}, respectively. The D-band of MWCNT shows a shift of 39 cm^{-1} with a change in excitation wavelength from 532 to 785 nm. In the case of MWCNTI, the shift towards lower wavenumber is by ~40 cm^{-1} with the same excitation wavelength change. The D-bands of MWCNTIIs and Carbotrap are shifted by ~38 and ~34 cm^{-1}, respectively towards lower wavenumber when the excitation wavelength is altered from 532 to 785 nm.

From the experimental observations, it is quite evident that the position and intensity of the D-band is different for various carbonaceous materials. It is a well-known fact that the position of D-band in the Raman spectrum appears at different wavenumbers with change in excitation wavelength. The band at ~1352 cm^{-1} is referred to as the main disorder-induced band (D1-band). This band occurs when disorder is present in the carbon aromatic structure. It is also sensitive to graphite intercalations. The change in the peak position of the D-band with excitation wavelength can be explained in terms of resonance of electronic and vibrational density of states. In carbonaceous materials, it has been observed that when phonon wavenumbers vary with a change in excitation energy,[15,24–26] a weak Raman signal is obtained.

The change of phonon wavenumbers with excitation wavelength is known as dispersive behaviour. In the present study, a shift of around ~40 cm^{-1} was observed for SWCNTs and the MWCNTs, when the excitation wavelength was changed as mentioned above (shift for the porous Carbotrap material was 34 cm^{-1}, while the graphite bar sample analysed showed a difference of 40 cm^{-1}). Evidently, the spectra obtained for 785-nm excitation showed significant D-band intensities for the SWCNT (CarboLex) and graphite samples when compared with the Raman spectra obtained with 532 nm. This is an important point to be noticed, when spectra in the literature are presented without stating the laser excitation wavelength. Thus the present study is a good example of the dispersive nature of different carbonaceous materials at different excitation wavelengths. In the carbonaceous materials, the D-band appears because of one-phonon second order Raman scattering process, for which elastic and inelastic scattering events are generally involved.[6,26,27]

In the Raman spectra of carbonaceous materials, the disorder mode is believed to result from disorder and symmetry lowering. In a study of SWCNT by Jorio *et al.*,[28] it has been reported that the D-band shows a strong dependence on the polarisation of the excitation wavelength. The polarisation dependence studies carried out earlier suggested that the observation of the D-band in the Raman spectrum of MWCNTs, where the D-band had been assumed to be associated with both the presence of disorder and finite size effect of carbons, did not always mean that it could originate only because of the disorder present in the material.

Recently, an optical study on CNTs and nanographites has been made by Pimenta *et al.*[29] In this study, it has been pointed out that the D-band also provides information about the size and orientation of the edges in nanographites. It has also been shown in this study that I_D/I_G for a given sample is strongly dependent on the laser energy and follows a dependence on E^{-4}_{laser}. The values of the ratio I_D/I_G calculated using the integrated intensities of the line profiles of the D- and G-bands, as shown in Fig. 3, for MWCNTI and MWCNTII are 0.31 and 0.55 for the excitation wavelength of 532 nm, and 0.79 and 1.51 for the excitation wavelength of 785 nm, respectively. The E^{-4}_{laser} dependence, taking the λ values of 532 and 785 nm, yields this ratio to be 0.211 as valid for nanographites. Our measurements for the special multi-walled varieties were made only for these two wavelengths, and differences may be obvious (the corresponding values were found to be 0.39 and 0.36 for MWCNTI and MWCNTII, respectively).

The D-band as characteristic for disordered graphite shows quite significant dependency of its intensity on the excitation wavelength. It is to be noted that this graphitic lattice vibration mode has been assigned to A_{1g} symmetry (refer also to spectra and the literature cited in Ref. [5]). In a recent review, Dresselhaus *et al.*[30] summarised the various aspects of Raman study, especially the variation of I_D/I_G ratio with the length of the SWCNTs and concluded that Resonance Raman spectroscopy (RRS) would become one of the major characterisation techniques for the specification of the CNT samples. It is evident from our study that a careful line shape analysis and determination of I_D/I_G for MWCNTS can provide information on the degree of CNT alignment. A comparison of the SEM micrographs of MWCNTI and MWCNTII clearly shows that the degree of alignment in case of MWCNTI is higher than that in case of MWCNTII (Fig. 2(a)). The values of I_D/I_G taking integrated G-band intensities have been calculated for each carbonaceous material at both the excitation wavelengths and are given in Table 2. In addition, the I_D/I_G ratio for each component of G-band was also calculated with the results reported in Table 2. It is obvious by a closer examination of these results that in the case of MWCNTI the value of the ratio I_D/I_G has a smaller value compared to the corresponding value for MWCNTII for the integrated G-band. Thus a relatively small value of the ratio I_D/I_G could be a very suitable parameter to monitor the degree of alignment in MWCNT bundles.

Raman G-band

The Raman spectra of different carbonaceous materials experimentally recorded in the region of 1750–1450 cm^{-1} show a composite nature of bands, which are assigned as G-band (G stands for 'graphite') originating from a first-order Raman effect. The overlap of the neighbouring D-band has been taken into account and subtracted before band fitting. A rigorous line shape analysis of the Raman line profiles corresponding to G-band for each carbonaceous material at two-excitation wavelengths, 532 and 785 nm, was performed taking widely varying initial guesses for three peaks. However, each start value finally yielded the same wavenumber positions for the three band components. During

Table 2. Peak positions, linewidths (FWHM) and I_D/I_G ratio for the Raman peaks of the G-band of different carbonaceous materials with two-excitation wavelengths

SWCNT	λ = 532 nm			λ = 785 nm			
ω (cm^{-1})	Width (cm^{-1})	$\frac{I_{1343}}{I_\omega}$	$\frac{I_{1343}}{I_G}$	ω (cm^{-1})	Width (cm^{-1})	$\frac{I_{1301}}{I_\omega}$	$\frac{I_{1301}}{I_G}$
1574	43	2.0	0.075	1555	58	0.54	0.185
1590	22	0.15		1582	21	0.42	
1605	21	0.16		1592	27	0.85	
MWCNT	**λ = 532 nm**			**λ = 785 nm**			
ω (cm^{-1})	Width (cm^{-1})	$\frac{I_{1347}}{I_\omega}$	$\frac{I_{1343}}{I_G}$	ω (cm^{-1})	Width (cm^{-1})	$\frac{I_{1308}}{I_\omega}$	$\frac{I_{1301}}{I_G}$
1564	22	9.5	1.04	1582	39	6.58	2.69
1580	28	3.08		1598	27	7.21	
1608	51	1.89		1613	22	12.36	
MWCNTI	**λ = 532 nm**			**λ = 785 nm**			
ω (cm^{-1})	Width (cm^{-1})	$\frac{I_{1352}}{I_\omega}$	$\frac{I_{1343}}{I_G}$	ω (cm^{-1})	Width (cm^{-1})	$\frac{I_{1312}}{I_\omega}$	$\frac{I_{1301}}{I_G}$
1580	30	0.88	0.31	1576	32	1.94	0.79
1590	31	0.66		1590	30	2.37	
1620	35	1.86		1612	26	3.08	
MWCNTII	**λ = 532 nm**			**λ = 785 nm**			
ω (cm^{-1})	Width (cm^{-1})	$\frac{I_{1354}}{I_\omega}$	$\frac{I_{1343}}{I_G}$	ω (cm^{-1})	Width (cm^{-1})	$\frac{I_{1316}}{I_\omega}$	$\frac{I_{1301}}{I_G}$
1587	30	0.66	0.55	1582	34	3.93	1.51
1606	23	8.23		1595	31	6.97	
1624	22	5.27		1617	31	3.78	
Carbotrap	**λ = 532 nm**			**λ = 785 nm**			
ω (cm^{-1})	Width (cm^{-1})	$\frac{I_{1344}}{I_\omega}$	$\frac{I_{1343}}{I_G}$	ω (cm^{-1})	Width (cm^{-1})	$\frac{I_{1301}}{I_\omega}$	$\frac{I_{1301}}{I_G}$
1575	33	1.13	0.80	1580	36	2.58	1.38
1590	28	6.20		1603	24	5.69	
1613	25	4.91		1615	20	6.21	
Graphite	**λ = 532 nm**			**λ = 785 nm**			
ω (cm^{-1})	Width (cm^{-1})	$\frac{I_{1354}}{I_{1587}}$	$\frac{I_{1343}}{I_G}$	ω (cm^{-1})	Width (cm^{-1})	$\frac{I_{1314}}{I_\omega}$	$\frac{I_{1301}}{I_G}$
1587	19	0.14	0.14	1582	20	0.87	0.80
				1613	20	9.4	

the fitting of the measured Raman line profile, each component band was assumed to be a mixture of a Lorentzian and a Gaussian profile. The fitting procedure takes the sum of Lorentzian and Gaussian fraction (in %), and the fitting routine *Spectra Calc* has a provision to adjust this ratio to calculate the best fit to the experimental line profile. Although the fitting is done by taking the sum of Lorentzian and Gaussian line shapes, a judicious mixture of the two profiles is nearly as good as a Voigt profile.[31]

Since we face much larger diameters for the outer tubes for typical MWCNT samples with most samples consisting of an ensemble of nanotubes with different diameters, the characteristic spectral differences that distinguish Raman spectra of SWCNTs from those of graphite are not so evident for MWCNTs. As there are different MWCNT varieties that have not been well investigated up to now, some new features were expected to be observed in the Raman spectra of the especially prepared MWCNT filter variety. Recently, Athalin and Lefrant[18] stated that only a single peak with a full width at half maximum (FWHM) larger 70 cm^{-1} would appear for MWCNT in contrast to the case of SWCNTs, which could be dismissed by our study.

The band system in the carbonaceous compounds studied, except for graphite, is composed of three peaks. Generally, the G-band in graphite with an undisturbed graphitic lattice (refer also our results in Table 2), nanocrystalline graphite or glassy carbon does not show dispersion.[3] The G-band shows a dispersive behaviour only for more disordered carbon, with dispersion proportional to the degree of disorder. Besides the first-order D-band, the spectra of our graphite bar sample also show another first-order band at ~1620 cm^{-1}, which is called D2-band and accounts for the structural disorders. Like the G-band of graphite, the D2-band also corresponds to a graphitic lattice mode with E_{2g} symmetry.[5] As found for the D1-band, the D2-band intensity also increases with larger excitation wavelength, which has been attributed to resonance effects.

A line shape analysis of the spectra of SWCNTs (Aldrich) yields three peaks at 1574, 1590 and 1607 cm^{-1} with 532-nm excitation, and at 1555, 1582 and 1590 cm^{-1} with 785-nm excitation. The results of the detailed line shape analysis for each carbonaceous material for both the excitation wavelengths are presented in Table 2. In a study by Reich *et al.*,[32] the intensities of Raman-active modes in single and multi-wall nanotubes have been investigated, elucidating that the Raman peaks are not due to modes of distinct, different symmetry, but a superposition of mainly A_1 and weaker E contributions.

The G-band in CNTs involves an optical phonon mode between the two dissimilar carbon atoms in a unit cell. It is known to originate from sp^2 carbon sites present in the sample.[1–3] This band essentially represents the ν(C=C) stretching vibration of all pairs of sp^2 atoms in the ring. According to group theoretical analysis, the G-band consists of six modes which are distributed as: 2A (A_{1g}), one doubly degenerate E_1 (E_{1g}) and another doubly degenerate E_2 (E_{2g}) mode. For each symmetrical mode, the vibration of atoms is either along the tube axis or along the circumferential direction. The peaks at ~1574 and ~1590 cm^{-1} for SWCNTs with excitation wavelength 532 nm belong to [$A(A_{1g}) + E_1(E_{1g})$] irreducible representation (IR) and the band at ~1607 cm^{-1} belongs to [$E_2(E_{2g})$] IR. The peaks at ~1574 and ~1590 cm^{-1} are equally shifted from the central graphite band at ~1582 cm^{-1} (actually measured here at 1587 cm^{-1}). These symmetry assignments have been supported by polarised Raman studies of semi-conducting SWCNTs in the earlier work of Jorio *et al.*[28]

The shifts have been explained using a model previously presented by Kasuya *et al.*[33] who considered that these modes appear at the Γ point of the nanotube Brillouin zone as a result of zone folding. Thus two bands at 1574 and 1590 cm^{-1} have equal separation of 8 cm^{-1} from the central graphite peak, ω_g = 1582 cm^{-1}. The third peak at ~1607 cm^{-1} is at double separation (~17 cm^{-1}) from the 1590 cm^{-1} peak and at triple separation (24 cm^{-1}) from the central graphite peak. The magnitude of the shift between the components of the G-band at two-excitation wavelengths may be due to the effect of impurities in the materials. However, these shifts in the peak positions

from the central graphite peak may also be the consequence of the nanotube curvature. The curvature of the nanotube results in different force constants along the nanotube axis and the circumferential direction. The nanotube geometry causes a force constant reduction along the tube axis compared to that in the circumferential direction. The curvature effect may, therefore, be responsible for the separation of $\Delta\nu = 24\,\mathrm{cm}^{-1}$ between the $A(A_{1g}) + E_1(E_{1g})$ and $E_2(E_{2g})$ modes. These peaks are reported at 1567, 1590 and 1607 cm^{-1} in the study on SWCNT carried out by Jorio *et al*.[28] If we look at Fig. 4(a), the G-band of SWCNTs is mainly consisting of two peaks at 1574 and 1590 cm^{-1}, which are assigned as G^- and G^+ bands, respectively. The G^+ feature is associated with carbon atom vibrations along the nanotube axis, known as longitudinal optical (LO) phonon mode in semi-conducting tubes, and its frequency is sensitive to a charge transfer mechanism. However, in case of metallic SWCNTs, the G^+ mode is associated with the transverse optical (TO) phonon. The G^- mode which originates from LO modes has Breit–Winger–Fano (BWF) line shape and it has been reported that the intensity of the G^- mode strongly depends on the chiral angle θ for metallic tubes.

The peak positions of the G^+ and G^- bands in SWCNTs with 785-nm excitation wavelength are 1582 and 1590 cm^{-1}, respectively. The G peak of the investigated SWCNTs with 785-nm excitation also splits into three band components at 1555, 1582 and 1590 cm^{-1} (Table 2). Thus the shift of the band at 1555 cm^{-1} from the central graphite peak amounts to 27 cm^{-1}. Compared to the spectrum recorded with 532-nm excitation, the band shifts and intensity differences make it impossible to have a symmetry assignment without further verification by polarised Raman scattering studies, although the peak at $\sim$1582 cm^{-1} matches nicely with the central graphite G-band belonging to $E_2(E_{2g})$ species. The assignment problem in the spectra of SWCNT and MWCNT has been discussed by Reich *et al*.[32] Besides the mixed symmetry of the bands, the band component corresponding to A species will be most intense.[28] In this context, it is noteworthy that a review on the symmetry-related properties of CNTs has been recently published by Barros *et al*.,[34] where excitonic effects have been taken into account, but Kohn anomaly effects have not been included. In a very recent study, Piscanec *et al*.[35] presented a review on the optical phonon dispersions of graphene and CNTs, where two Kohn anomalies induced by the electron–phonon coupling of E_{2g} mode at Γ point and A_1' mode at K point were discussed using an approach accounting for the time-independent nature of phonons, which was usually neglected in the Born–Oppenheimer framework.

An important aspect of the G-band is the Raman line shape which differs in accordance with the metallic or semi-conducting nature of the nanotube. In general, in other sp^2 carbons, the G-band is not dispersive, i.e. its wavenumber is not sensitive to the excitation wavelength.[2] In the present study, however, we observed a shift in wavenumber position of both G^+ and G^- bands with a change of excitation wavelength, which might be also caused by some impurities present in the sample. The G^- and G^+ modes with 532 nm excitation appear at 1574 and 1590 cm^{-1}, respectively and at 1555 and at 1590 cm^{-1}, respectively, with 785-nm excitation. It clearly shows that the G^- mode is downshifted by $\sim$19 cm^{-1} with a change of excitation wavelength from 532 nm to the longer wavelength of 785 nm. On the other hand, the G^+ mode does not show any significant shift on varying the excitation wavelength. In the Raman spectra of isolated semi-conducting CNTs, the G^- and G^+ modes show Lorentzian character.[31] However, both modes show different features for metallic CNTs. In the case of SWCNTs, the G^+ mode shows Lorentzian lineshape with relatively small linewidth (FWHM = 21 cm^{-1}) while the G^- peak shows a line shape with a relatively large width (FWHM = 48 cm^{-1}). In the present study, both G^+ and G^- bands could be fitted nicely using Lorentzian line shape functions. The linewidths of G^- and G^+ modes obtained were 48 and 22 cm^{-1}, respectively (Table 2), where the band of the lower Raman shift mode showed further broadening with an increase in excitation wavelength. Nonetheless, the SWCNTs used in the present study are predominantly semi-conducting in character.

Multi-walled CNTs can be considered as an ensemble of nanotubes with diameters ranging from small to rather large. Because of the large diameters of the outer shells for MWCNT, most differences that can be utilised to distinguish between the Raman spectra of SWCNT and graphite are missing in MWCNTs. In our study, a Lorentzian line shape analysis of the Raman spectra for all MWCNTs and the microporous Carbotrap material in the region 1750–1450 cm^{-1} for both excitation wavelengths, 532 and 785 nm, was carried out, and each spectrum was fitted, as mentioned earlier, taking three peaks into account. The results obtained are presented in Table 2. Multiple splittings of G-band modes were observed for individual MWCNTs by Zhao *et al*.,[36] who stated that for verifying the symmetry assignments, polarised Raman scattering studies would be needed. A polarised Raman study of aligned MWCNTs has been reported by Rao *et al*.[37] Furthermore, an interesting study on the influence of the diameters in the Raman spectra of multi-walled aligned CNTs has been very recently reported by Antunes *et al*.[38]

A further close examination of the MWCNT data presented in Table 2 reveals a marked difference between the MWCNT and the filter varieties. A small difference between the Aldrich MWCNT and the two filter varieties is that the G-bands in the Aldrich MWCNT exhibit a small dispersive behaviour, whereas MWCNTI and MWCNTII show almost no dispersion with the change in the excitation wavelength. The dispersive nature of the G-band is associated with the Kohn anomaly effect, which is more pronounced in the case of metallic tubes. However, this aspect is under very active study, but it is still not well understood. The positions of the three peaks are found at 1568, 1584, and 1610 cm^{-1} with 532-nm excitation wavelength. However, these three peaks are shifted to 1580, 1590 and 1615 cm^{-1} in MWCNTI and to 1581, 1592 and 1624 cm^{-1} in the case of MWCNTII. Furthermore, the ratio I_D/I_G, where I_D and I_G are the intensities of the D- and G-bands, is also presented in Table 2 for each carbonaceous material. In the case of the MWCNT commercial sample, the three peaks are relatively narrow at 532-nm excitation wavelength, while for both MWCNTI and MWCNTII filters, these peaks are slightly broader.

Surprisingly, the Raman spectra of the Carbotrap material also show a spectral feature similar to that of CNTs. There is a trend with the highest frequency band component appearing more prominently when one follows the series MWCNTI, MWCNTII and porous carbon black sample. The prominence of the $G^+ - G^-$ doublet is more evident in the spectra obtained with 785-nm excitation. The intensities of D- and G-bands and their positions in the cases of the MWCNT and Carbotrap materials change with excitation laser wavelength, whereas the G-band in our graphite

Table 3. Peak positions, linewidths (FWHM), and relative intensities for the two component Raman peaks of the G′-band of different carbonaceous materials with two-excitation wavelengths

	λ = 532 nm			λ = 785 nm		
Sample	ω (cm^{-1})	Width (cm^{-1})	Intensity (arb. units)	ω (cm^{-1})	Width (cm^{-1})	Intensity (arb. units)
SWCNT	2623	80	74.7	2579	79	88.1
	2675	72	72.4			
MWCNT	2663	19	45.5	2571	134	82.4
	2685	35	26.3	2613	71	127.0
MWCNTI	2640	47	58.2	2566	33	62.3
	2698	58	51.4	2616	56	38.6
MWCNTII	2705	52	58.2	2619	54	59.6
Carbotrap	2641	76	69.5	2608	68	59.2
	2685	67	77.8			
Graphite	2688	57	44.9	2608	80	54.8
	2725	43	63.2	2649	53	83.5

sample also shows similar dispersion accounting for a slight degree of disorder in the material.[3]

Raman G′-band

A Lorentzian line shape analysis of the Raman spectra for the different carbonaceous materials, recorded in the region, 2800–2400 cm^{-1}, has been done and the measured spectra along with the fitted peaks for the two-excitation wavelengths, 532 and 785 nm, are presented in Figs 4(b) and 5(b), respectively. The spectra of the different carbonaceous materials in the region, 2800–2400 cm^{-1} show one broad band assigned to the G′-band. The G′-band in the Raman spectra of all the carbonaceous materials, with both 532 and 785-nm excitation wavelengths, mainly shows a double band nature with a few exceptions, and they are analysed taking two peaks into consideration. The results of this fitting have been presented in Table 3. In a recent study by Shimada *et al.*,[39] the origin of the 2450 cm^{-1} Raman band in highly ordered pyrolytic graphite (HOPG), single-wall and double-wall carbon nanotubes has been discussed. The band at 2450 cm^{-1} shows no dispersion, whereas the G′-band is highly dependent on E_{laser}. However, we have concentrated mainly on MWCNTs, where the 2450 cm^{-1} band could not be seen in the measured spectra. A more detailed study is perhaps required to explore this Raman band. In a more recent study also, Barros *et al.*[40] have extended their Raman study for characterising graphitic foams, wherein by analysing the dependence of the G′ band line shape on the excitation energy, it was found that the G′ band line shape was strongly correlated with the presence of stacking faults.

The G′-peak observed in the Raman spectra of all the carbonaceous materials, which is basically the second harmonic of the D1-band, appears at $\sim 2\omega_D$ wavenumber position, when sp^2 bonded carbon atoms are present.[6,35] This peak exhibits a strong dispersive behaviour as a function of excitation energy. The intense band of the analysed SWCNTs spectrum shows a shift of 44 cm^{-1} upon change of excitation wavelength from 532 to 785 nm. On the other hand, the most intense band of MWCNTs shows a shift of ~85 cm^{-1} upon increasing the excitation wavelength. This clearly implies that the MWCNT materials are showing a strong dispersive nature compared to the SWCNT material investigated.

The double peak nature in the G′-peak has been explained in terms of double resonance process in which the electronic energy state matches with the excitation energy.[6] In 2D graphite, the D-band originates from the TO phonon branch close to the K point in the Brillouin zone. Both D- and G′-peaks are sensitive to the diameter and chirality of the CNTs. Apart from this, the features of the D- and G′- bands are found to change according to how the 2D electronic phonon structure is folded into a 1D structure. Along with the dependence on diameter and chirality of the tube, it also shows a strong dependence on excitation wavelength in the present study. The double peak nature of the G′-mode arises from the Van Hove singularities occurring at the electronic joint density of states.[6,21,41] The two peaks in the G′-band for SWCNTs and MWCNTs arise because of the resonance with two different Van Hove singularities of the same nanotube occurring independently for both the incident and scattered photons. The origin of G′-peaks, as shown in Figs 4(b) and 5(b) can be associated with phonon modes corresponding to the wave vector $q = 2k$. In the 3D carbonaceous materials, say graphite, the double peak nature of G′-band is due to inter-layer coupling.[6] However, this mechanism is not applicable for SWCNTs and MWCNTs, since they do not basically possess a 3D structure.

Conclusions

The Raman spectra of different carbonaceous materials were recorded using two different excitation wavelengths, and the most prominent band structures are analysed and compared. The D-band in the Raman spectra of different carbonaceous materials, which results because of disorder and symmetry lowering, exhibits a significant dispersive behaviour with change of excitation wavelength. The G-band of the carbonaceous materials except graphite consists of six modes. For each symmetrical mode in the nanotubes, the vibration of atoms is either along the tube axis or along the circumferential direction, which is designated as G^+ or G^- bands, respectively. In case of SWCNTs, these two components are fitted using a Lorentzian line shape function, where the broad band feature essentially confirms that the SWCNTs used in the present study are predominantly semi-conducting in nature. The G- and D2- bands of the other materials are also investigated for their dispersive behaviour with a closer look at the MWCNT and Carbotrap species. The stable Raman shift position of the triplet band system for the MWCNT filter species, nearly independent from the two-excitation wavelengths, is a unique result of our investigation. Further studies are under way, for which the range of laser wavelengths will be extended (e.g. 488 and 1064 nm).

While studying the band intensities, it was found that the G-band in the spectral features of the MWCNTI filter species dominated over the D-band for both excitation wavelengths, similar to that of the SWCNT varieties studied in this work. On the other hand, relatively less aligned MWCNTII species showed a spectral similarity much closer to that of the microporous graphitised carbon black material, providing clues on the disordered structures. On the basis of the results of this study, the intensity ratio, I_D/I_G may be used as a measure of the degree of MWCNT alignment, and thus Raman spectroscopy may prove to be a reliable and quick method of quality control during fabrication of aligned MWCNTs. The G′-band of the other carbonaceous materials exhibits a double band nature, which is not observed in the case of MWCNT filters (for MWCNTI only a weak component exists). For the CNT filter materials, the SEM study revealed evidently the formation of

highly aligned arrays of bundles of CNTs, for which the Raman spectra showed unique features compared to other carbonaceous materials studied.

Acknowledgements

The Nordrhein-Westfalen and Financial support by the Ministerium für Innovation, Wissenschaft und Forschung des Landes Nordrhein-Westfalen and the Bundesministerium für Bildung und Forschung is gratefully acknowledged by two authors (H.M.H., R.K.). The authors would like to thank Dr Lijie Ci for helping in the HRTEM study and Prof. P.M. Ajayan for permitting us to use the facility and also for his valuable suggestions. The authors are thankful to Prof. O.N. Srivastava for initiating our interest in this field. One of the authors (A.S.) is thankful to the UGC and DST, New Delhi. Two of us (AKO and BPA) are grateful to the Alexander von Humboldt Foundation, Germany for research support, which helped in initiating this collaboration. The authors would also like to thank the reviewer for giving valuable suggestions.

References

[1] Y. Wang, D. C. Alsmeyer, R. L. McCreery, *Chem. Mater.* **1990**, *26*, 557.
[2] A. C. Ferrari, I. Robertson, *Phys. Rev. B* **2001**, *64*, 075414.
[3] A. C. Ferrari, *Diamond Relat. Mater.* **2002**, *11*, 1053.
[4] M. Kawakami, T. Karato, T. Takenaka, S. Yokoyama, *ISIJ Int.* **2005**, *45*, 1027.
[5] A. Sadezky, H. Muckenhuber, H. Grothe, R. Niessner, U. Pöschl, *Carbon* **2005**, *43*, 1731.
[6] M. S. Dresselhaus, G. Dresselhaus, R. Saito, A. Jorio, *Phys. Rep.* **2005**, *409*, 47.
[7] S. Iijima, T. Ichihashi, *Nature (London)* **1993**, *363*, 603.
[8] D. S. Bethune, C. H. Klang, M. S. De Vries, G. Gorman, R. Savoy, J. Vazquez, R. Beyers, *Nature (London)* **1993**, *363*, 605.
[9] S. Iijima, *Nature (London)* **1991**, *354*, 56.
[10] M. S. Dresselhaus, M. Endo, *Carbon Nanotubes: Synthesis, Structure, Properties and Applications*, *Topics in Applied Physics*, vol. 80 (Eds: M. S. Dresselhaus, G. Dresselhaus, P. Avouris), Springer: Berlin, **2001**, pp 11.
[11] Y. Ando, X. Zhao, T. Sugai, M. Kumar, *Mater. Today* **2004**, *7* (October issue) 22.
[12] K. Awasthi, A. Srivastava, O. N. Srivastava, *J. Nanosci. Nanotechnol.* **2005**, *5*, 1616.
[13] C. N. R. Rao, R. Sen, B. C. Satishkumar, A. Govindararaj, *Chem. Commun.* **1998**, *15*, 1525.
[14] A. Srivastava, O. N. Srivastava, S. Talapatra, R. Vajtai, P. M. Ajayan, *Nat. Mater.* **2004**, *3*, 610.
[15] C. Thomsen, S. Reich, *Phys. Rev. Lett.* **2000**, *85*, 5214.
[16] M. S. Dresselhaus, G. Dresselhaus, A. Jorio, A. G. Filho, R. Saito, *Carbon* **2002**, *40*, 2043.
[17] A. Jorio, M. A. Pimenta, A. G. Filho, R. Saito, G. Dresselhaus, M. S. Dresselhaus, *New J. Phys.* **2003**, *5*, 139.
[18] H. S. Athalin, A. Lefrant, *J. Raman Spectrosc.* **2005**, *36*, 400.
[19] M. Valcárcel, B. M. Simonet, S. Cárdenas, B. Suárez, *Anal. Bioanal. Chem.* **2005**, *382*, 1783.
[20] M. Kruk, K. M. Kohlhaas, B. Dufour, E. B. Celer, M. Jaroniec, K. Matyjaszewski, R. S. Ruoff, T. Kowalewski, *Microporous Mesoporous Mater.* **2007**, *102*, 178.
[21] P. Tan, S. Dimovski, Y. Gogotsi, *Philos. Trans. R. Soc. London, Ser. A* **2004**, *362*, 2289.
[22] C. Thomsen, S. Reich, J. Maultzsch, *Philos. Trans. R. Soc. London, Ser. A* **2004**, *362*, 2337.
[23] K. Kneipp, H. Kneipp, M. S. Dresselhaus, S. Lefrant, *Philos. Trans. R. Soc. London, Ser. A* **2004**, *362*, 2361.
[24] J. Kurti, V. Zolyomi, A. Gruneis, H. Kuzmany, *Phys. Rev. B* **2002**, *65*, 165433.
[25] R. Saito, A. Gruneis, G. G. Samaonidge, V. W. Brar, G. Dresselhaus, M. S. Dresselhaus, A. Jario, L. G. Cyncado, C. Fantini, M. A. Pimenta, A. G. Souza Filho, *New J. Phys.* **2003**, *5*, 157.1.
[26] R. Saito, A. Jorio, A. G. Souza Filho, G. Dresselhaus, M. S. Dresselhaus, M. A. Pimenta, *Phys. Rev. Lett.* **2002**, *88*, 027401.
[27] R. Saito, G. Dresselhaus, M. S. Dresselhaus, *Physical Properties of Carbon Nanotubes*, Imperial College Press: London, **1998**.
[28] A. Jorio, G. Dresselhaus, M. S. Dresselhaus, M. Souza, M. S. S. Dantas, M. A. Pimenta, A. M. Rao, R. Saito, C. Liu, H. M. Cheng, *Phys. Rev. Lett.* **2000**, *85*, 2617.
[29] M. A. Pimenta, A. P. Gomes, C. Fantini, L. G. Cancado, P. T. Araujo, I. O. Maciel, A. P. Santos, C. A. Furtado, V. S. T. Peressinotto, F. Plentz, A. Jorio, *Physica E* **2007**, *37*, 88.
[30] M. S. Dresselhaus, G. Dresselhaus, M. Hofmann, *Vib. Spectrosc.* **2007**, *45*, 71.
[31] B. P. Asthana, W. Kiefer, *Appl. Spectrosc.* **1982**, *36*, 250.
[32] S. Reich, C. Thomsen, G. S. Duesberg, S. Roth, *Phys. Rev. B* **2001**, *63*, 041401.
[33] A. Kasuya, Y. Sasaki, Y. Saito, K. Tohji, Y. Nishina, *Phys. Rev. Lett.* **1997**, *78*, 4434.
[34] E. B. Barros, A. Jorio, G. G. Samsonidze, R. B. Capaz, A. G. S. Filho, J. M. Filho, G. Dresselhaus, M. S. Dresselhaus, *Phys. Rep.* **2006**, *431*, 261.
[35] S. Piscanec, M. Lazzeri, F. Mauri, A. C. Ferrari, *Eur. Phys. J. Spec. Top.* **2007**, *148*, 159.
[36] X. Zhao, Y. Ando, L.-C. Qin, H. Kataura, Y. Maniwa, R. Saito, *Appl. Phys. Lett.* **2002**, *81*, 2550.
[37] A. M. Rao, A. Jorio, M. A. Pimenta, M. S. S. Dantas, R. Saito, G. Dresselhaus, M. S. Dresselhaus, *Phys. Rev. Lett.* **2000**, *84*, 1820.
[38] E. F. Antunes, A. O. Lobo, E. J. Corat, V. J. Trava-Airoldi, *Carbon* **2007**, *45*, 913.
[39] T. Shimada, T. Sugai, C. Fantini, M. Souza, L. G. Cancado, A. Jorio, M. A. Pimenta, R. Saito, A. Grüneis, G. Dresselhaus, M. S. Dresselhaus, Y. Ohno, T. Mizutani, H. Shinohara, *Carbon* **2005**, *43*, 1049.
[40] E. B. Barros, A. G. S. Filho, H. Son, M. S. Dresselhaus, *Vib. Spectrosc.* **2007**, *45*, 122.
[41] M. J. Matthews, M. A. Pimenta, G. Dresselhaus, M. S. Dresselhaus, M. Endo, *Phys. Rev. B* **1999**, *59*, R6585.

